# Mobile Assemblies of Bricard Linkages Inspired from Waterbomb Thick-Panel Origami

Xiao Zhang(✉) and Yan Chen

School of Mechanical Engineering, Tianjin University, Tianjin 300072, China
zhangxiaofun@tju.edu.cn

**Abstract.** Mobile assemblies of spatial linkages and thick-panel origami patterns have been used to design deployable structures for aerospace, such as solar arrays and antennas. The kinematic equivalence between a mobile assembly and thick-panel form has been used to design new of them based on the known assemblies and origami patterns. Here, waterbomb origami pattern is taken as the research object, and two types of plane-symmetric Bricard linkages are derived from the **D** and **W** thick-panel origami vertices, where linkages and thick-panel vertices are kinematically equivalent. Furthermore, new mobile assemblies of plane-symmetric Bricard linkages are constructed by using the transition method based on the multi-vertex waterbomb thick-panel origami pattern, and a special type mobile assembly with two motion paths is derived under the specific geometric conditions. A prototype is manufactured and two motion paths are verified according to the deployment sequences. This work proposes a bridge between waterbomb thick-panel origami and the assembly of plane-symmetric Bricard linkages and shows the possibility of design morphing assembly of linkages.

**Keywords:** Waterbomb origami · Bricard linkage · Mobile assembly

## 1 Introduction

Mobile assemblies of linkages are networks of unit linkages [1], which have great potential for engineering applications, such as shelters [2, 3], antennas [4, 5] and backbone for solar panels [6]. Based on typical unit linkages, such as Bennett linkages, Myard linkages and Bricard linkages, multiple mobile assemblies are constructed according to the tessellation method [7] and movable connection method [8]. These assemblies have different deployed configurations, such as planes [9], arches [7], parabolic cylindrical surfaces [10] and polyhedrons [11–13]. However, there is a limited number of mobile assemblies based on Bricard linkages due to the complex motion.

On the other hand, rigid origami patterns are generally kinematically equivalent to mobile assemblies of spherical linkages [14] and they have been used to be transited to new mobile assemblies of spatial linkages by regarding the thick-panel forms to bridges [1, 15]. These thick-panel forms are constructed based on the offset-crease method where four-crease, five-crease and six-crease vertices are kinematically equivalent to Bennett linkage, Myard linkage, Bricard linkage, respectively [16], which indicates a


N. V. Khang et al. (Eds.): ASIAN MMS 2021, MMS 113, pp. 101–108, 2022.
https://doi.org/10.1007/978-3-030-91892-7_10

multi-vertex thick-panel form is kinematically equivalent to multi-linkage assembly. By now, four-crease origami patterns and diamond origami patterns have been used to design mobile assemblies of Bennett linkages and mobile assemblies of plane-symmetric Bricard linkages, correspondingly [1, 15]. As waterbomb is a typical origami pattern consists of two types of six-crease origami vertices, it indicates the thick-panel form can be used to design a new assembly of Bricard linkages [17]. In addition, the geometric conditions about two motion paths of the waterbomb thick-panel origami [17] show the potential to construct a mobile assembly to realise morphing.

This paper aims at constructing mobile assemblies of plane-symmetric Bricard linkages from waterbomb thick-panel origami. The layout of the paper is listed as follows. Section 2 proposes two types of plane-symmetric Bricard linkages from vertices of waterbomb thick-panel origami. In Sect. 3, an assembly of plane-symmetric Bricard linkages with two paths is transited from multi-vertex waterbomb thick-panel origami. Conclusions are drawn with further discussion in Sect. 4.

## 2 Bricard Linkages Derived from Two Types of Six-Crease Vertices

A waterbomb origami pattern consists of two types of six-crease vertices, **D** type and **W** type. A crease pattern with eight **D** type vertices and ten **W** type vertices is shown in Fig. 1(a) where solid lines are mountain creases and dashed lines are valley creases. Its motion sequences under plane-symmetric conditions are shown in Fig. 1(b).

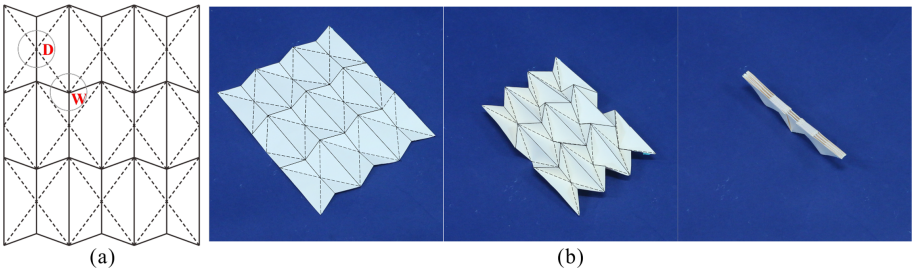


**Fig. 1.** A waterbomb origami. (a) The crease pattern with **D** and **W** types of vertices. (b) Motion sequences under plane-symmetric conditions of each vertex.

Figure 2(a) shows an enlarged vertex **D** with axes marked along the creases by $z_i$ ($i = 1, 2, \ldots, 6$) and sector angles noted by $\alpha_{12} = \alpha_{34} = \alpha_{45} = \alpha_{61} = \alpha$ and $\alpha_{23} = \alpha_{56} = \pi - 2\alpha$ ($0 < \alpha \leq \pi/2$) to satisfy the flat foldability. Under the plane-symmetric condition, its thick-panel form can be constructed based on the offset-crease method, as shown in Fig. 2(b), which is corresponding to a plane-symmetric Bricard linkage [16]. To achieve the compact folding without interference, thicknesses of six panels satisfy

$$t_{12}^{\mathrm{D}} = t_{23}^{\mathrm{D}} = t_{34}^{\mathrm{D}} = t_{45}^{\mathrm{D}} = t_{56}^{\mathrm{D}} = t_{61}^{\mathrm{D}} = (2 + \mu)a, \tag{1}$$

where $\mu = \cos(\alpha + \beta) \sin\alpha / \sin\beta$ and another solution is $\mu = 1$ when $\alpha = \beta$ under compatibility conditions for waterbomb thick-panel form [17].

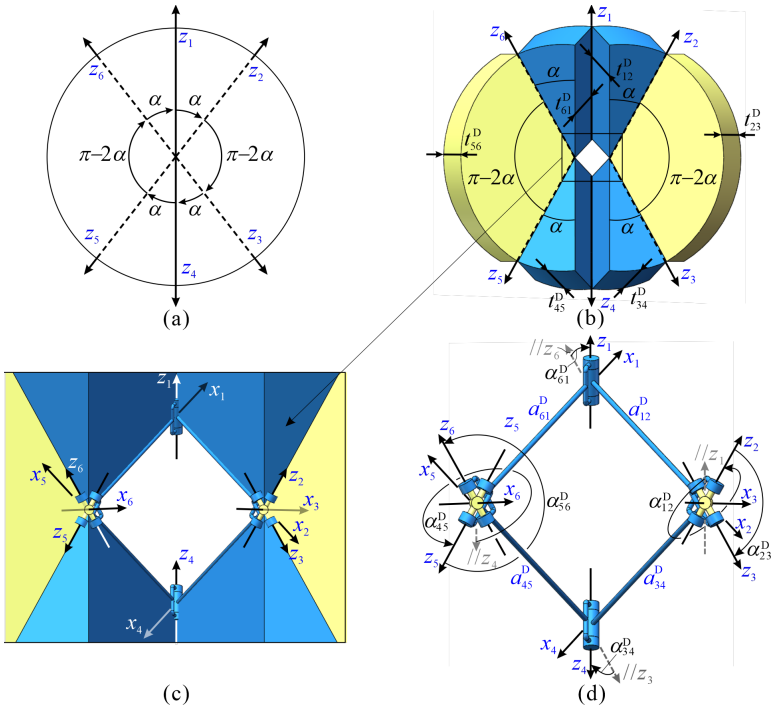


**Fig. 2.** The **D** type vertex and its corresponding Bricard linkage. (a) The crease pattern. (b) The corresponding thick-panel form and (c) the enlarged vertex. (d) The corresponding Bricard linkages with D-H notations.

The coordinate systems according to the Denavit and Hartenberg (D-H) notation [18] are marked in Fig. 2(c). By replacing the thick panels with links and connecting the adjacent revolute joints along the shortest distance, the corresponding plane-symmetric Bricard linkage is constructed in Fig. 2(d) with marked link lengths and twists. Hence, the single-vertex thick-panel origami in Fig. 2(c) and the special plane-symmetric Bricard linkage in Fig. 2(d) are kinematically equivalent. The relationships between twists of the linkage and sector angles of the origami vertex can be obtained as

$$\alpha_{12}^{\mathbf{D}} = -\alpha_{61}^{\mathbf{D}} = -\alpha, \quad \alpha_{23}^{\mathbf{D}} = -\alpha_{56}^{\mathbf{D}} = \pi - 2\alpha, \quad \alpha_{34}^{\mathbf{D}} = -\alpha_{45}^{\mathbf{D}} = \alpha, \tag{2}$$

and that between thicknesses of panels and lengths of links are

$$a_{12}^{\mathbf{D}} = a_{34}^{\mathbf{D}} = a_{45}^{\mathbf{D}} = a_{61}^{\mathbf{D}} = t_{12}^{\mathbf{D}} = (2+\mu)a, \quad a_{23}^{\mathbf{D}} = a_{56}^{\mathbf{D}} = 0. \tag{3}$$

For the vertex **W** of waterbomb pattern in Fig. 3(a), six axes $z_i$ ($i = 1, 2, \ldots, 6$) are marked along the creases with sector angles $\alpha_{12} = \alpha_{61} = \pi - \alpha - \beta$, $\alpha_{23} = \alpha_{56} = \beta$ and $\alpha_{34} = \alpha_{45} = \alpha$, where $0 < \alpha, \beta \leq \pi/2$. Similar to the **D** vertex, its thick-panel form can be constructed by offsetting hinges, as shown in Fig. 3(b). To obtain the compact folding property and flat unfolded profile, the thickness of panels satisfies

$$t_{12}^{\mathbf{W}} = t_{61}^{\mathbf{W}} = (1+\mu)a, \; t_{23}^{\mathbf{W}} = t_{56}^{\mathbf{W}} = a, \; t_{34}^{\mathbf{W}} = t_{45}^{\mathbf{W}} = \mu a, \; t'_{12} = t'_{61} = (2+\mu)a. \tag{4}$$

The enlarged thick-panel vertex in Fig. 3(c) shows the construction of the corresponding plane-symmetric Bricard linkage. Similar to the **D** vertex, the theoretical links connected to hinges are along the direction of the common normal of the adjacent axes, and the kinematic equivalence between single-vertex thick-panel origami in Fig. 3(c) and the plane-symmetric Bricard linkage in Fig. 3 (d) can be easily obtained.

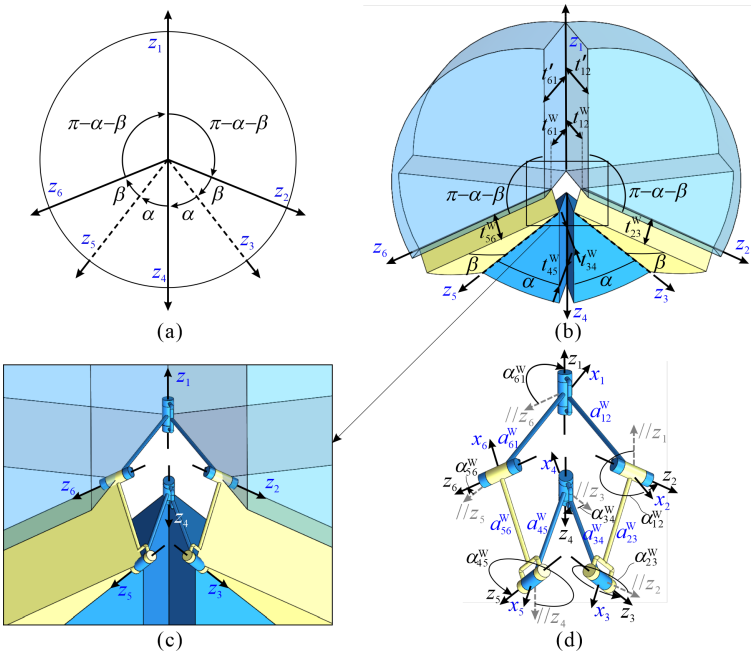


**Fig. 3.** The **W** type vertex and its corresponding Bricard linkage. (a) The crease pattern. (b) The corresponding thick-panel form and (c) the enlarged vertex. (d) The corresponding Bricard linkages with D-H notations.

According to the notations of the origami vertex and the linkage, relationships between twists of the linkage and sector angles of the origami vertex are

$$\alpha_{12}^{\mathbf{W}} = -\alpha_{61}^{\mathbf{W}} = \alpha + \beta - \pi, \quad \alpha_{23}^{\mathbf{W}} = -\alpha_{56}^{\mathbf{W}} = -\beta, \quad \alpha_{34}^{\mathbf{W}} = -\alpha_{45}^{\mathbf{W}} = \alpha. \tag{5}$$

To ensure the flat foldability of **W** thick-panel vertex, relationships between the thickness of panels and lengths of links satisfy

$$a_{12}^{\mathbf{W}} = a_{61}^{\mathbf{W}} = t_{12}^{\mathbf{W}} = t_{61}^{\mathbf{W}} = (1+\mu)a, \; a_{23}^{\mathbf{W}} = a_{56}^{\mathbf{W}} = t_{23}^{\mathbf{W}} = t_{56}^{\mathbf{W}} = a, \; a_{34}^{\mathbf{W}} = a_{45}^{\mathbf{W}} = t_{34}^{\mathbf{W}} = t_{45}^{\mathbf{W}} = \mu a. \tag{6}$$

## 3 Mobile Assemblies of Bricard Linkages from Multi-vertex Waterbomb Thick-Panel Origami

Figure 4(a) is the representative portion of a waterbomb pattern consisting of four vertices A, B, C, D with creases noted by $a_i$, $b_i$, $c_i$, $d_i$ ($i = 1, 2,\ldots, 6$) and sector angles marked by $\alpha$, $\beta$, $\pi - 2\alpha$, $\gamma = \pi - \alpha - \beta$. Figure 4(b) shows the corresponding thick-panel form which indicates an assembly of two types of plane-symmetric Bricard linkages. For panel $P_1$, it is connected to three linkages A, B, D with links $a_{34}$, $b_{12}$, $d_{23}$, as shown in Fig. 4(c). The shared joints between linkages A and D, linkages B and D, linkages A and B, i.e., $a_3/d_3$, $b_2/d_2$ and $a_4/b_1$, are combined into one. Then a closed loop is constructed based on the links and joints from $a_3/d_3$ to $a_4/b_1$ via $a_{34}$, through $b_{12}$ to $b_2/d_2$, and then back to $a_3/d_3$ by $d_{23}$. Along the thickness direction of the panel $P_1$, the order of joints, $a_4/b_1$ in the bottom, $b_2/d_2$ in the middle and $a_3/d_3$ on the top are determined, respectively. The link lengths satisfy

$$a_{34}^{\mathrm{A}} = b_{12}^{\mathrm{B}} + d_{23}^{\mathrm{D}} = (2 + \mu)a. \tag{7}$$

Similarly, the order of joints in the panel $P_2$ can be obtained as $d_1/c_1$, $b_2/d_2$ and $b_3/c_6$. When transit panels to be links, the arrangement of joints on a link can be determined by the order of joints in the panels. Hence, a mobile assembly of plane-symmetric Bricard linkages corresponding to the waterbomb thick-panel origami is constructed, as shown in Fig. 4(d). From Eqs. (2), (3), (5), (6) and (7), construction conditions of the mobile assembly of plane-symmetric Bricard linkages can be derived, as

$$\begin{aligned}
&\alpha_{12}^{\mathrm{A}} = \alpha_{12}^{\mathrm{C}} = -\alpha,\ \alpha_{23}^{\mathrm{A}} = \alpha_{23}^{\mathrm{C}} = \pi - 2\alpha,\ \alpha_{34}^{\mathrm{A}} = \alpha_{34}^{\mathrm{C}} = \alpha,\\
&\alpha_{12}^{\mathrm{B}} = \alpha_{12}^{\mathrm{D}} = \alpha + \beta - \pi,\ \alpha_{23}^{\mathrm{B}} = \alpha_{23}^{\mathrm{D}} = -\beta,\ \alpha_{34}^{\mathrm{B}} = \alpha_{34}^{\mathrm{D}} = \alpha,\\
&a_{34}^{\mathrm{A}} = b_{12}^{\mathrm{B}} + d_{23}^{\mathrm{D}},\ c_{61}^{\mathrm{C}} = b_{23}^{\mathrm{B}} + d_{12}^{\mathrm{D}},\ k_{34}^{\mathrm{K}} = k_{23}^{\mathrm{K}} + k_{12}^{\mathrm{K}},
\end{aligned} \tag{8}$$

where $k$ and K represent $a$, $b$, $c$, $d$ and A, B, C, D or **D** and **W**, respectively.

The angles $\alpha_{45}$, $\alpha_{56}$, $\alpha_{61}$ and link lengths $k_{45}$, $k_{56}$, $k_{61}$ can be easily obtained based on Eqs. (2), (3), (5), (6) and (7). When $\mu = 1$, $\alpha + \beta < \pi/2$, $\alpha = \beta$, there are always two smooth folding paths [17]. Here, we arbitrarily choose a pattern with six vertices (Fig. 5) whose parameters satisfy $\mu = 1$ and $\alpha = \beta = 40^\circ$ in Eq. (9). Two motion sequences of the prototype are shown in Fig. 5. Here, Fig. 5(a) shows the planar motion path of thick-panel origami from the flat configuration to the closed pack configuration, and the mobile assembly corresponds to the path from a bundle to a strip via the intermediate configuration. Similarly, Fig. 5(b) shows the arch motion path of thick-panel origami and the corresponding motion of mobile assembly of Bricard linkages. The curves of relationships of kinematic variables $\varphi_i$ and $\phi_i$ ($i = 1, 2$) can be derived from Eqs. (10) and (11) [17], as shown in Fig. 5(c). The deployed configuration i and folded configuration ii of thick-panel origami are with $\varphi_i = \phi_i = 180^\circ$ and $\varphi_i = \phi_i = 0$, respectively. Here, $\varphi_i$ and $\phi_i$ are dihedral angles corresponding to crease $i$ of thick-panel origami vertices **D** and **W**, respectively.

$$\begin{aligned}
&\alpha_{12}^{\mathrm{A}} = \alpha_{12}^{\mathrm{C}} = \alpha_{12}^{\mathrm{E}} = -\alpha = -40^\circ,\ \alpha_{23}^{\mathrm{A}} = \alpha_{23}^{\mathrm{C}} = \alpha_{23}^{\mathrm{E}} = 100^\circ,\ \alpha_{34}^{\mathrm{A}} = \alpha_{34}^{\mathrm{C}} = \alpha_{34}^{\mathrm{E}} = \alpha = 40^\circ,\\
&\alpha_{12}^{\mathrm{B}} = \alpha_{12}^{\mathrm{D}} = \alpha_{12}^{\mathrm{F}} = -20^\circ,\ \alpha_{23}^{\mathrm{B}} = \alpha_{23}^{\mathrm{D}} = \alpha_{23}^{\mathrm{F}} = -\beta = -40^\circ,\ \alpha_{34}^{\mathrm{B}} = \alpha_{34}^{\mathrm{D}} = \alpha_{34}^{\mathrm{F}} = \alpha = 40^\circ,
\end{aligned}$$

$$
\begin{aligned}
&a_{34}^{\mathrm{A}} = b_{12}^{\mathrm{B}} + d_{56}^{\mathrm{D}} = 3a,\ c_{61}^{\mathrm{C}} = b_{23}^{\mathrm{B}} + d_{45}^{\mathrm{D}} = 3a,\\
&a_{12}^{\mathbf{D}} = c_{12}^{\mathbf{D}} = e_{12}^{\mathbf{D}} = 3a,\ a_{23}^{\mathbf{D}} = c_{23}^{\mathbf{D}} = e_{23}^{\mathbf{D}} = 0,\ a_{34}^{\mathbf{D}} = c_{34}^{\mathbf{D}} = e_{34}^{\mathbf{D}} = 3a,\\
&b_{12}^{\mathbf{W}} = d_{12}^{\mathbf{W}} = f_{12}^{\mathbf{W}} = 3a,\ b_{23}^{\mathbf{W}} = d_{23}^{\mathbf{W}} = f_{23}^{\mathbf{W}} = 0,\ b_{34}^{\mathbf{W}} = d_{34}^{\mathbf{W}} = f_{34}^{\mathbf{W}} = 3a.
\end{aligned}
\tag{9}
$$

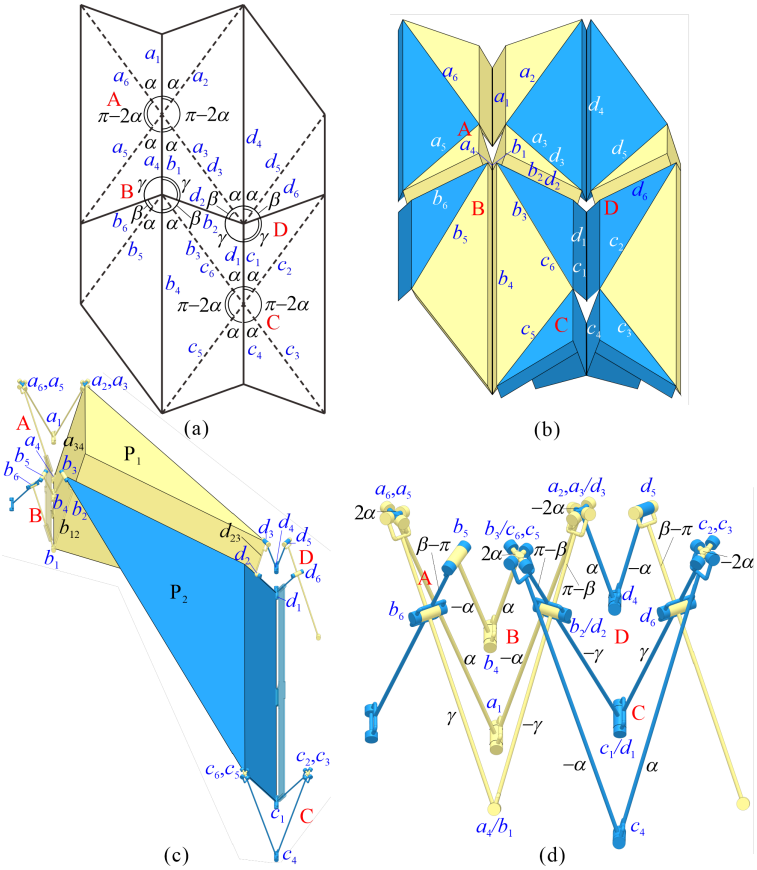


**Fig. 4.** The transition of multi-vertex waterbomb pattern. (a) Crease pattern with four vertices, where $\gamma = \pi - \alpha - \beta$. (b) Its thick-panel form. (c) The enlarged view of the two shared panels with four attached plane-symmetric Bricard linkages and (d) the corresponding mobile assembly with four Bricard linkages.

$$
\tan\frac{\varphi_1}{2} = \frac{1}{\cos\alpha}\tan\frac{\varphi_2}{2},\ \varphi_4 = \varphi_1,\ \varphi_2 = \varphi_3 = \varphi_4 = \varphi_5 = \varphi_6. \tag{10}
$$

$$
\tan\frac{\phi_1}{2} = \frac{1}{\cos\alpha}\tan\frac{\phi_3}{2},\ \tan\frac{\phi_2}{2} = \frac{\cos(\alpha+\beta)}{\cos\alpha}\tan\frac{\phi_3}{2},\ \phi_4 = \phi_1,\ \phi_5 = \phi_3,\ \phi_6 = \phi_2. \tag{11a}
$$

$$\tan\frac{\phi_1}{2} = \frac{\tan(\phi_3/2)\left(\sin^2(\alpha+\beta)\tan^2(\phi_3/2) + 2\left(\sin^2\beta + \sin^2\alpha\right)\right)}{\sin(\alpha+\beta)(\sin\beta + \cos(\alpha+\beta)\sin\alpha)\tan^2(\phi_3/2) + 4\sin\alpha\sin\beta\cos\beta},$$
$$\tan\frac{\phi_2}{2} = \frac{\sin(\alpha+\beta)}{2\sin\alpha}\tan\frac{\phi_3}{2},\ \phi_5 = \phi_3, \phi_6 = \phi_2,$$
$$\tan\frac{\phi_4}{2} = \frac{\tan(\phi_3/2)\left(4\sin\alpha\sin^2(\alpha+\beta)\tan^2(\phi_3/2) - 8\sin\alpha\left(2\sin^2\beta - \sin^2(\alpha+\beta)\right)\right)}{(\cos(3\alpha+\beta) - 8\cos(\alpha+\beta) + 7\cos(\alpha-\beta))\sin(\alpha+\beta)\tan^2(\phi_3/2) + 8\sin^2\alpha\sin 2\beta}, \tag{11b}$$

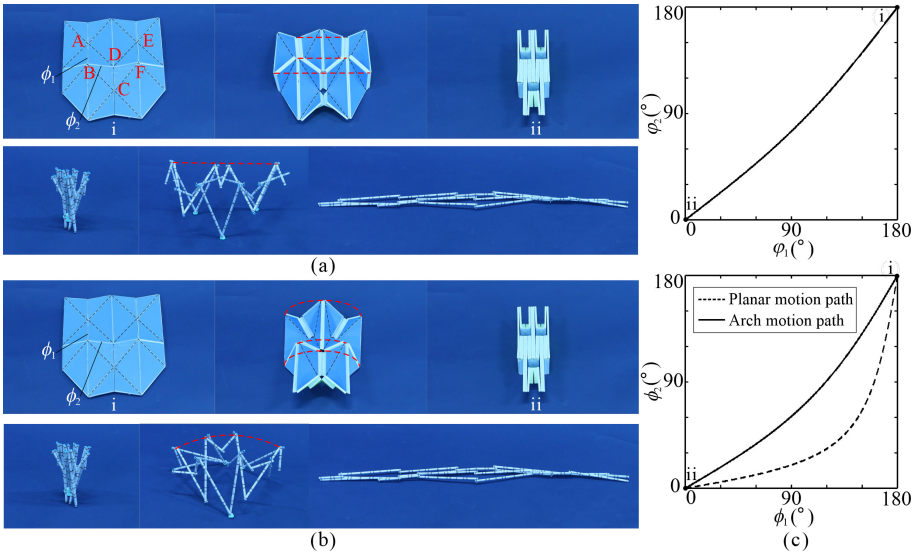


**Fig. 5.** Two paths of motion sequences of a waterbomb thick-panel origami and its corresponding mobile assembly of plane-symmetric Bricard linkages with $\alpha = \beta = 40°$. (a) The planar motion sequences. (b) The arch motion sequences. (c) The curves of $\varphi_2$ vs. $\varphi_1$ and $\phi_2$ vs. $\phi_1$.

## 4 Conclusions

In this paper, new mobile assemblies consisting of two types of plane-symmetric Bricard linkages have been constructed from waterbomb thick-panel origami based on their kinematic equivalence. According to the geometric conditions in the reference [17], waterbomb thick-panel origami with two smooth paths is constructed. By transiting the thick-panel form to a mobile assembly, the morphing mobile assembly is created, which has the planar deploying movement and the arch deploying movement. The two paths can be changed at the position where mobile assembly is in the fully folded configuration with all links in a line.

As the **D** type vertex is a line- and plane-symmetric origami vertex, we can conjuncture that this vertex can generate thick-panel origami kinematically equivalent to a line-symmetric Bricard linkage. The waterbomb thick-panel pattern with the **D** type vertex and plane-symmetric **W** type vertex could be transited to an assembly mixed with

line-symmetric Bricard linkages and plane-symmetric Bricard linkages. This study also can be extended to the thick-panel forms from other six-crease rigid origami patterns, such as the Resch pattern. Furthermore, new mobile assemblies of spatial linkages can be obtained by our proposed approach.

## References

1. Zhang, X., Chen, Y.: Mobile assemblies of Bennett linkages from four-crease origami patterns. Proc. Roy. Soc. A-Math. Phys. Eng. Sci. **474**, 20170621 (2018)
2. De Temmerman, N., Mollaert, M., Mele, V., et al.: Design and analysis of a foldable mobile shelter system. Int. J. Space Struct. **22**, 161–168 (2007)
3. Alegria Mira, L., Thrall, A.P., De Temmerman, N.: Deployable scissor arch for transitional shelters. Automat. Constr. **43**, 123–131 (2014)
4. You, Z.: Deployable structure of curved profile for space antennas. J. Aerosp. Eng. **13**, 139–143 (2000)
5. Cui, J., Huang, H., Li, B., Deng, Z.: A novel surface deployable antenna structure based on special form of Bricard linkages. In: Dai, S.J., Zoppi, M., Kong, X. (eds.) Advances in Reconfigurable Mechanisms and Robots I, pp. 783–792. Springer, London (2012)
6. Xu, Y., Lin, Q., Wang, X., Li, L., Cong, Q., Pan, B.: Mechanism design and dynamic analysis of a large-scale spatial deployable structure for space mission. In: 7th International Conference on Electronics and Information Engineering, p. 1032226. SPIE, Nanjing (2017)
7. You, Z., Chen, Y.: Motion Structures: Deployable Structural Assemblies of Mechanisms. Spon Press, New York (2014)
8. Huang, H., Deng, Z., Li, B.: Mobile assemblies of large deployable mechanisms. J. Space Eng. **5**, 1–14 (2012)
9. Ma, B., Huang, H.: Large deployable networks constructed by interconnected Bricard linkages. Adv. Mater. Res. **338**, 723–726 (2011)
10. Song, X., Deng, Z., Guo, H., Liu, R., Li, L., Liu, R.: Networking of Bennett linkages and its application on deployable parabolic cylindrical antenna. Mech. Mach. Theory **109**, 95–125 (2017)
11. Yang, F., You, Z., Chen, Y.: Mobile assembly of two Bennett linkages and its application to transformation between cuboctahedron and octahedron. Mech. Mach. Theory. **145**, 103698 (2020)
12. Xiu, H., Wang, K., Wei, G., Ren, L., Dai, J.: A Sarrus-like overconstrained eight-bar linkage and its associated Fulleroid-like platonic deployable mechanisms. Proc. Inst. Mech. Eng. C-J. Mech. Eng. Sci. **234**, 241–262 (2020)
13. Chen, Y., Yang, F., You, Z.: Transformation of polyhedrons. Int. J. Solids. Struct. **138**, 193–204 (2018)
14. Dai, J.S., Rees Jones, J.: Mobility in metamorphic mechanisms of foldable/erectable kinds. J. Mech. Design **121**, 375–382 (1999)
15. Zhang, X., Chen, Y.: The diamond thick-panel origami and the corresponding mobile assemblies of plane-symmetric Bricard linkages. Mech. Mach. Theory **130**, 585–604 (2018)
16. Chen, Y., Peng, R., You, Z.: Origami of thick panels. Science **349**, 396–400 (2015)
17. Chen, Y., Feng, H., Ma, J., Peng, R., You, Z.: Symmetric waterbomb origami. Proc. Roy. Soc. A-Math. Phys. Eng. Sci. **472**, 20150846 (2016)
18. Denavit, J., Hartenberg, R.S.: A kinematic notation for lower-pair mechanisms based on matrices. Trans. ASME J. Appl. Mech. **22**, 215–221 (1955)